Electronic structure of stoichiometric and off-stoichiometric TaC_x

G. H. Schadler and A. M. Boring
Los Alamos National Laboratory, Los Alamos, New Mexico 87545

P. Weinberger
Institut für Technische Elektrochemie, Technical University of Vienna, A-1060 Vienna, Austria

A. Gonis
Lawrence Livermore National Laboratory, Livermore, California 94550

(Received 19 February 1988)

We have determined the electronic structure of stoichiometric and substoichiometric TaC by means of the relativistic Korringa-Kohn-Rostoker Green's-function method. The introduction of vacancies was treated within the coherent-potential approximation. We find that the main difference between the ordered and disordered compound is a charge transfer from the nonmetal to the metal atom. Additional vacancy states (−3.0 eV below the Fermi energy) play a minor role. We calculate x-ray photoemission spectroscopy (XPS) intensities for both stoichiometric and substoichiometric cases and find (unlike previous calculations) excellent agreement with the XPS data. We also compare our results with the measured linear specific-heat coefficient and find that the sharp drop seen in this quantity with increasing vacancy concentration cannot be explained by our results.

I. INTRODUCTION

The understanding of the electronic structure of group-IV*B* and -V*B* transition-metal monocarbides and mononitrides has been of quite some interest. These alloys show a tendency to have their properties change dramatically when they become substoichiometric. They are also of technical interest because of their hardness that seems to depend on vacancy concentration. Some of these properties can be understood by considering the electronic structure. The stoichiometric compounds are fairly well understood theoretically as well as experimentally. Several efforts have also been undertaken to determine the electronic structure for substoichiometric titanium and niobium carbides and nitrides. As was found by x-ray photoemission spectroscopy (XPS) experiments and later confirmed by the nonrelativistic Korringa-Kohn-Rostoker coherent-potential approximation (KKR CPA) calculations by Klima *et al.*[1] and Marksteiner *et al.*,[2] the introduction of vacancies in these systems gives rise to new states that modify significantly the density of states (DOS). This was also found by Redinger *et al.*[3] for $TiC_{0.75}$ using the augmented plane-wave (APW) method by introducing vacancies at a specific site. These results were in contradiction to some earlier tight-binding calculations[4] that predicted only small changes in the DOS due to charge transferred back from the nonmetal atom to the metal atom. Because vacancy states are not really included in the tight-binding CPA method it was felt that this method could not explain the changes in the electronic structure of these materials upon changing vacancy concentrations.

As mentioned above, there have been studies of the electronic structure of these materials by means of XPS spectra for titanium carbide[5,6] (group IV*B*) and niobium carbide[7] (group V*B*). The increased XPS intensities 1–2 eV below the Fermi energy (E_F) could be interpreted as additional vacancy states in the substoichiometric compounds. Recently there has been a thorough investigation on substoichiometric tantalum carbide (TaC_x) by Gruzalski and Zehner.[8] They determined core-level binding energies and the valence-band structure of TaC_x ($0.5 < x < 1.0$) by x-ray photoelectron spectroscopy. They found an increasing XPS intensity around 1–2 eV below E_F and also a shift of the main peak towards E_F with increased vacancy concentration. They also interpreted this increased XPS intensity as due to vacancy states as had been found in the lighter carbides by nonrelativistic KKR CPA calculations. The only available theoretical DOS for TaC_x was from a tight-binding CPA calculation by Klein *et al.*[9] Again this study gave similar results for TaC_x as were found by the tight-binding CPA on the lighter carbides. Because no KKR CPA results existed for TaC_x the question of the importance of charge transfer as opposed to vacancy-state contributions to the changes in the electronic structure could not be resolved. Also, because the tight-binding CPA calculated DOS does not agree with recent XPS data their results could be questioned. (Their calculation misses the first peak below E_F.) For these reasons it seemed reasonable to perform a fully relativistic KKR CPA calculation that included vacancy-state contributions for TaC_x.

Also, the comparison of the theoretical electronic structure to experimental data has recently been enhanced by improvements in making these alloys. As described by Gruzalski *et al.*[8] they have now been able to tightly control the composition of TaC_x by a new sample growing technique. The XPS technique is quite useful for

probing DOS since it uses high-energy photons that penetrate deeper into the sample than do surface-type photoemission techniques and therefore is a better measure of the bulk DOS. At these high energies a simplified theoretical expression for the intensity can be formulated (see below). For the interpretation of the spectra in terms of the basic electronic structure one has to look at two factors, namely the energy dependence of the cross sections and the DOS. In this work we have calculated both of these quantities so a better comparison between theory and experiment can be made. Unfortunately, sometimes the poor instrumental resolution puts some restrictions on the experimental technique and misses many of the details of the calculated electronic structure.

Another quantity generally used to compare the calculated DOS with is the linear specific-heat coefficient γ that for simple metals ordinarily is considered to be proportional to the DOS at E_F. Experimentally γ shows a sharp decrease with increasing vacancy concentration for TaC_x.[10] The earlier tight-binding calculations of Klein *et al.*[9] found an increasing DOS at the Fermi energy with increasing vacancy concentration. A discussion for possible reasons for this discrepancy can also be found in Ref. 9. Again, because of these shortcomings a more elaborate calculation seemed to be necessary to clarify the influence of vacancies on the electronic structure of TaC_x.

In this paper we will first adopt the fully relativistic Korringa-Kohn-Rostoker coherent-potential approximation (RKKR CPA) method to calculate the DOS of the stoichiometric and the substoichiometric TaC (with 28% vacancy concentration of the carbon site). A relativistic formulation of the KKR CPA theory was given by Staunton *et al.*[11] and Weinberger *et al.*[12] for cubic crystals with one atom per unit cell. Since TaC_x crystallizes in the sodium chloride structure (two atoms per unit cell, $a_0=8.39047$ a.u.) we generalized the RKKR CPA method in the same way as was done by Klima *et al.*[1] for the nonrelativistic case. The major problem is the increase in the size of the matrices involved, so that it becomes computationally much more tedious. Having calculated the DOS we then calculate the XPS spectra for the stoichiometric and substoichiometric compound.

First we discuss the generalization of the RKKR CPA theory from one atom per unit cell to many atoms per unit cell in the relativistic case. Section III deals with computational details. In Sec. IV we describe the DOS and follow that with a discussion of the experimental as well as theoretical XPS spectra. Finally we present our conclusions.

II. THEORETICAL CONSIDERATIONS

As was shown by Klima *et al.*[1] and Schadler *et al.*[13] the generalization of the Korringa-Kohn-Rostoker Green's-function (KKR GF) method from one atom per unit cell to more atoms per unit cell is quite straightforward. For the relativistic case the same formalism carries over. One just uses a different representation (spin-spherical harmonics) for the angular and spin parts of the functions. For a thorough discussion of the relativistic formulation of the KKR GF method for one atom per unit cell see Staunton *et al.*[11] and Weinberger *et al.*[12,14] Here we just give the final result for the DOS in terms of the fully relativistic cell and site diagonal scattering path operator $\tau^{i_s i_s}_{QQ'}(E)$, where $Q=(\kappa,\mu)$ are the relativistic quantum numbers, s and s' are the indices of the sublattice, and the unit cell Ω_i is partitioned into subcells Ω_{i_s} such that $\Omega_i=\sum_s \Omega_{i_s}$:

$$\tau^{i_s i_{s'}}_{QQ'}(E)=\int_{\Omega_{BZ}} \tau^{i_s i_{s'}}_{QQ'}(E,\mathbf{k})d\mathbf{k} , \tag{1}$$

where

$$\tau^{i_s i_{s'}}_{QQ'}(E,\mathbf{k})=[t^{i_s}_{QQ'}(E)^{-1}\delta_{ss'}-G^{i_s i_{s'}}_{QQ'}(E,\mathbf{k})]^{-1} , \tag{2}$$

and $t^{i_s}_{QQ'}(E)$ is the single-site t matrix and $G^{i_s i_{s'}}_{QQ'}(E,\mathbf{k})$ are the well-known relativistic structure constants (Onodera and Okazaki[15]) as obtained in terms of the nonrelativistic structure constants for complex lattices (Segall[16]) and $\delta_{ss'}$ denotes the Kronecker symbol. The first-order density matrix can be written as

$$n^i(E,\mathbf{r})=-\frac{1}{\pi}\sum_s \mathrm{Im}[G^{i_s i_s}(E,\mathbf{r},\mathbf{r})] , \tag{3}$$

where the Green's function is given in terms of the scattering path operator by (see Faulkner[17] and Weinberger *et al.*[14])

$$G^{i_s j_{s'}}(E,\mathbf{r},\mathbf{r}')=\sum_{QQ'} Z^{i_s}_Q(E,\mathbf{r})\tau^{i_s j_{s'}}_{QQ'}(E)Z^{j_{s'}}_Q(E,\mathbf{r}') - \sum_Q Z^{i_s}_Q(E,\mathbf{r})J^{j_{s'}}_Q(E,\mathbf{r}') \tag{4}$$

and where $Z^{i_s}_Q(E,\mathbf{r})$ and $J^{i_s}_Q(E,\mathbf{r})$ are normalized atomic wave functions as defined in Ref. 14.

The DOS is found by integrating Eq. (3) over the volume of the unit cell, whereas the charge density is obtained by integrating Eq. (3) over the energy from $-\infty$ up to the Fermi energy E_F. Local partial DOS are easily obtained by taking the corresponding angular spin projections of Eq. (3).

A relativistic formulation for the XPS intensities in the framework of density-functional theory has been given by Marksteiner *et al.*[18] using scattering formalism. A simple formula for the angular integrated intensity of the XPS spectrum was derived as

$$I(E+\omega)=\sum_s \sum_Q \sigma^{i_s}_Q(E+\omega)n^{i_s}_Q(E) , \tag{5}$$

where $n^{i_s}_Q(E)$ are the partial local DOS [Eq. (3)] for each site and each quantum number Q. The $\sigma^{i_s}_Q(E+\omega)$ are the relativistic cross sections for a fixed photon energy ω ($=1486.6$ eV for the Al $K\alpha$ line) evaluated over the band energies E. Equation (3) was used to determine the Fermi energy E_F and the DOS functions $n^{i_s}_Q(E)$. Equation (5) makes transparent the connection between the electronic structure and the experimental photoemission data. The cross sections include selection rules as well as information about the crystal potential and therefore are not merely constant factors but vary from compound to compound.

III. COMPUTATIONAL DETAILS

In order to calculate the Brillouin-zone (BZ) integral in Eq. (1) we used ten special directions as given by Fehlner *et al.*[19] for complex energies with a constant imaginary part of 0.01 Ry for the substoichiometric compound and 0.03 Ry for the ordered compound. The scattering path operator and scattering amplitude were then deconvoluted back to the real energy axis as described by Klima *et al.*[1] As is discussed therein the introduction of a small imaginary part smooths the integrand of Eq. (1). Therefore no sharp peaks show up in the DOS. The integrated DOS itself is within usual accuracy. For the ordered compound we used fully relativistic self-consistent potentials of TaC as obtained by Weinberger *et al.*[20] For the vacancy potential a superposition process was performed with overlapping tantalum and carbon atomic potentials adjusted to the muffin-tin values of the self-consistent calculation for TaC. The RKKR CPA calculation itself was not performed self-consistently with respect to the one-electron charge density. This is of course a drawback, but as will be seen, the overall features of the DOS and XPS spectra agree reasonably well with the experimental results so it seems unnecessary to perform an expensive self-consistent calculation for this compound. In addition, as was discussed by Klima *et al.*,[1] the self-consistent determination of the vacancy potential seems to be not important. The energy dependence of the $l=0$ phase shift of the vacancy varies only a little with energy and it is negative for positive energies. The importance of the self-consistency for the Ta and C in the substoichiometric compound cannot be addressed here. We hope in future to be able to perform self-consistent calculations.

IV. DENSITY OF STATES FOR TaC AND $TaC_{0.72}$

In Fig. 1 we show the total DOS for TaC (solid line) and $TaC_{0.72}$ (dashed line). The Fermi energy E_F is zero. The introduction of vacancies on the carbon sublattice reduces the number of states around -4.5 eV and creates additional states around -1 eV. Figures 2 and 3 show the component projected DOS of TaC and $TaC_{0.72}$, respectively. As one can see in both cases there is a lot of hybridization between Ta and C. The DOS of the vacancy is rather small and does not show up in the total DOS as was found for lighter carbides. The partial local DOS are mainly $5d$-like for tantalum and $2p$-like for carbon as can be seen from Figs. 4 and 5 (note: the $2s$ states of carbon are further down in energy and are not shown).

Comparing in Figs. 2 and 3 the stoichiometric with the substoichiometric compound one can see that there is a reduction of the carbon contribution around -4.5 eV which is due to the fact that only 72% of the carbon lattice sites are occupied. The decrease of the DOS for the tantalum around -4.5 eV displays the fact that we do not get a rigid band behavior but a redistribution of states due to the introduction of randomly distributed vacancies at the carbon sites resulting in breaking some of the p—d

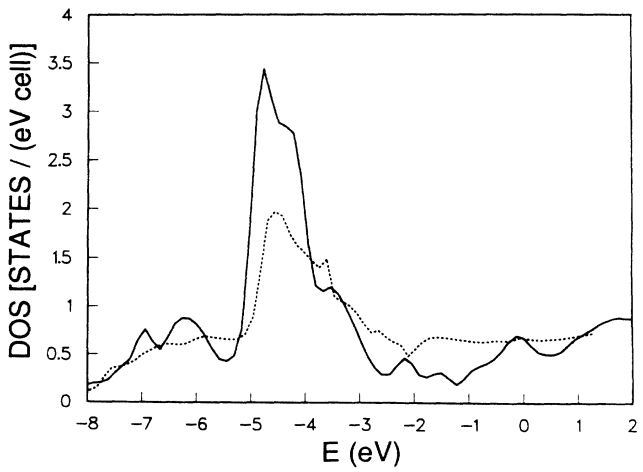

FIG. 1. Total density of states (DOS) for TaC (solid line) and $TaC_{0.72}$ (dashed line). E_F is at 0.

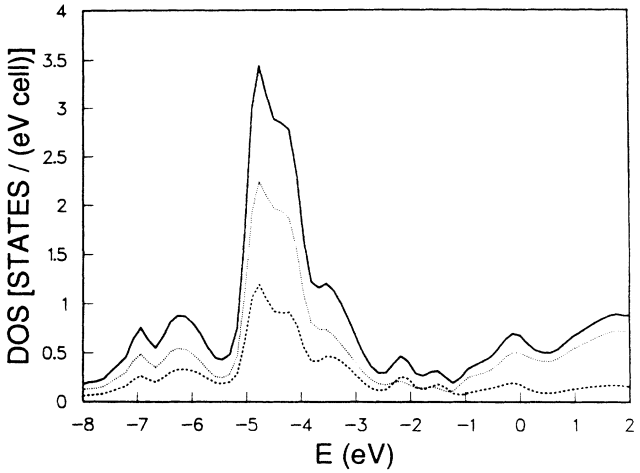

FIG. 2. Total (solid line) and component DOS (Ta, dotted line; C, dashed line) for TaC. E_F is at 0.

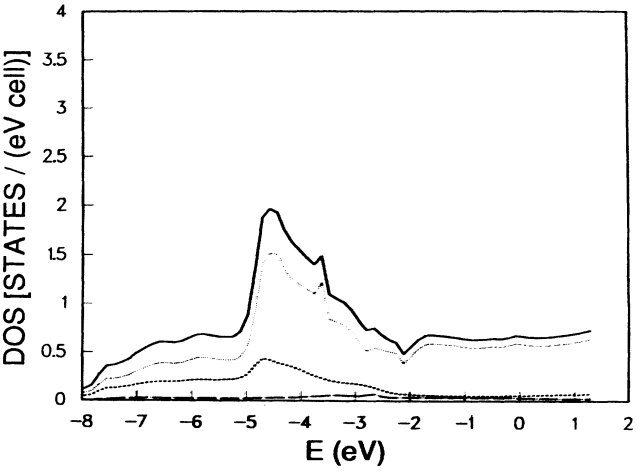

FIG. 3. Total (solid line) and components DOS (Ta, dotted line; C, dashed line and chain dotted line for the vacancy) for $TaC_{0.72}$. E_F is at 0.

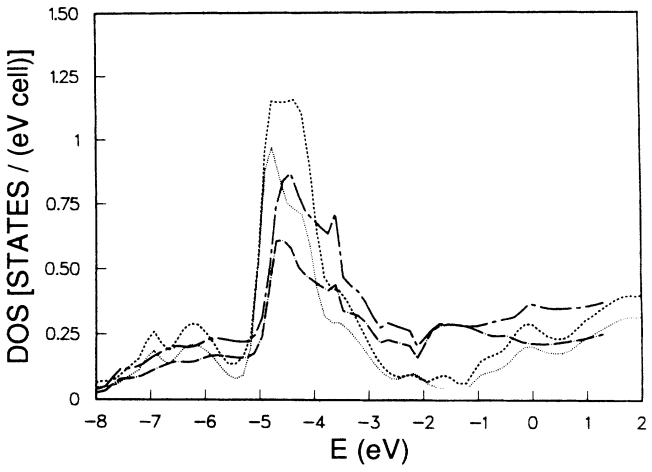

FIG. 4. $5d(\Gamma_8^+)$ and $5d(\Gamma_7^+)$-like local partial DOS for Ta in TaC (dotted and dashed line, respectively) and $TaC_{0.72}$ (chain-dotted and chain-dashed line, respectively). E_F is at 0.

bonds. Going in energy towards E_F one sees a decrease in the carbon DOS but also an increase in the tantalum contribution [especially for the $5d(\Gamma_7^+)$-like states]. Looking at the integrated DOS for the different components (Table I) we find charge transferred back from the carbon site to tantalum in going to the substoichiometric compound as was found by Klein *et al.*[9] Although such comparisons are always troublesome because of the question of how to partition the unit cell, we think these numbers are still useful because the unit cell was partitioned in the same manner for both cases. The total numbers are also questionable since our calculation is not performed self-consistently with respect to the one-electron charge densities. But at least the trend should be right. This rather large shift of tantalum states from lower energies (with respect to the Fermi energy) to higher ones is quite different from the nonrelativistic

TABLE I. Charge around each site along with the density of states at the Fermi energy $n(E_F)$ for TaC_x.

x	Ta	C	Vacancy	$n(E_F)$
1.00	4.47	4.53		9.29
0.72	4.89	2.78	0.21	9.11

KKR CPA results for the lighter carbide and nitride compounds and in agreement with the tight-binding CPA results for TaC_x. Also we find only a small contribution from the additional vacancy states (around -3 eV; see Fig. 6) in contrast to the nonrelativistic KKR CPA results for TiC_x and TiN_x. In these systems the vacancy states are found just (1–2 eV) below (or above) the Fermi energy and are also seen in the experimental data. The last column in Table I gives the DOS at E_F. We find a more or less constant DOS with increasing vacancy concentration.

V. XPS SPECTRA

We performed a calculation of the XPS intensities and compared it to the findings of Gruzalski *et al.*[8] In order to calculate the total integrated intensities of the XPS spectra we calculated the scattering cross sections for the different elements Figure 7 shows the cross sections for tantalum. The *s*-like cross sections for carbon are around 1 (arbitrary units) and the *p*-like ones are about 0.1 on the scale of Fig. 7 and are not displayed. Also the cross sections for the vacancy are essentially zero. From Figs. 7 and 4 it is seen that the main features in both the stoichiometric as well as the substoichiometric compound are given by the tantalum $5d$-like contributions. Their cross sections are big and they dominate the DOS. Although the Ta *p*-like cross sections are almost twice as big as the Ta *d*-like cross sections, the Ta *p*-like partial DOS is very small. Therefore taking the product of these two quantities gives only a small contribution to the total XPS intensity. To account for the finite instrument reso-

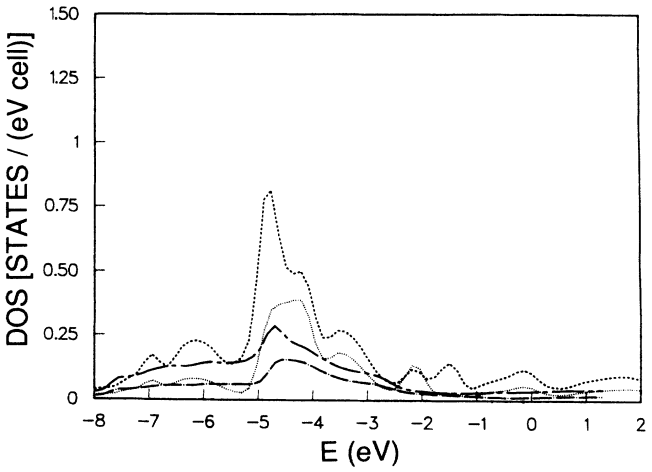

FIG. 5. $2p_{1/2}$ and $2p_{3/2}$ local partial DOS for C in TaC (dotted and dashed line, respectively) and $TaC_{0.72}$ (chain-dotted and chain-dashed line, respectively). E_F is at 0.

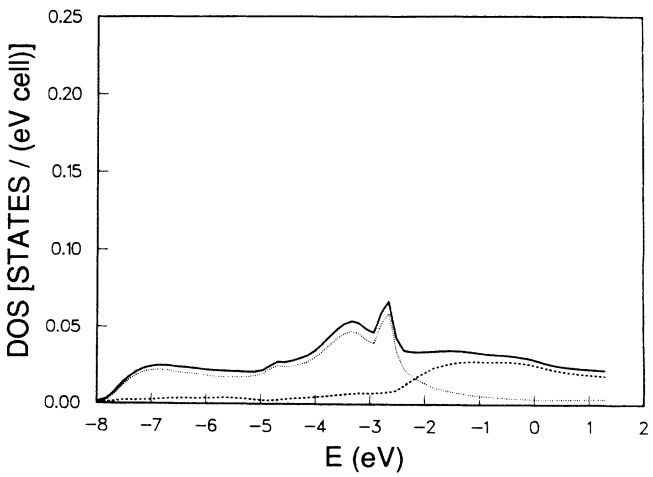

FIG. 6. Vacancy total DOS (solid line), *s*-like (dotted line), and *p*-like (dashed line) local partial DOS. E_F is at 0.

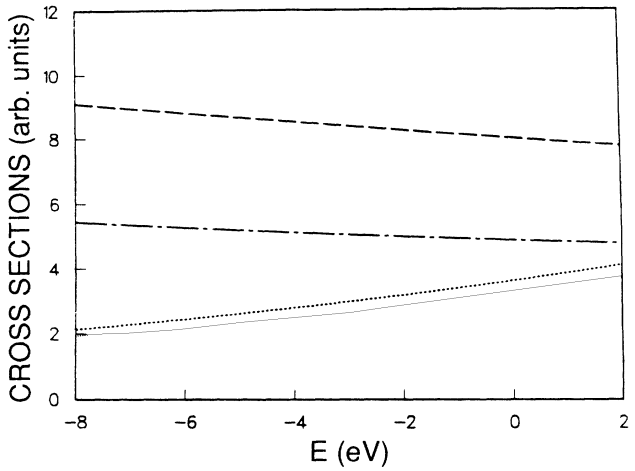

FIG. 7. Ta cross sections for $d_{3/2}$ (dotted line), $d_{5/2}$ (dashed line), $p_{1/2}$ (chain-dotted line), and $p_{3/2}$ (chain-dashed line). The value of the C cross sections for s is around 1, whereas for p about 0.1. The amount for the vacancy cross sections is essentially zero.

lution we assumed the same values for the broadening as was used in Ref. 8, namely a Gaussian with a half-width at half maximum of 1.2 eV. We get fairly good agreement between the experiment and theory. A comparison to previous similar calculations for lighter transition-metal carbides (see Redinger *et al.*[21]) shows that our calculation agrees better with the experiment than comparisons found in this paper. The positions of the peaks (with respect to E_F) in the experimental spectra for the stoichiometric compound (Fig. 8, solid line) are -5.28 eV (A) and -0.97 eV (B) and for the substoichiometric alloy (Fig. 8, dashed line) -4.8 eV (A') whereas it is hard to determine the position of the shoulder around -2 eV (B'). The values in the theoretical spectrum are -4.55 eV (A) and -0.5 eV (B) for the stoichiometric system (Fig. 9, solid line) and -4.2 eV (A') and around

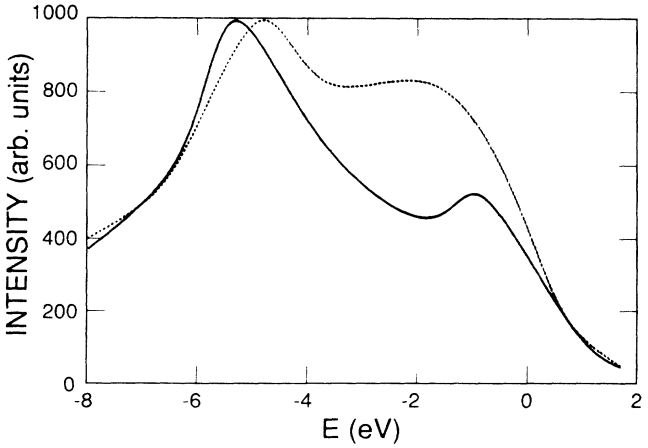

FIG. 8. Experimental XPS spectra for TaC (solid line) and $TaC_{0.72}$ (dotted line) from Ref. 8. E_F is at 0.

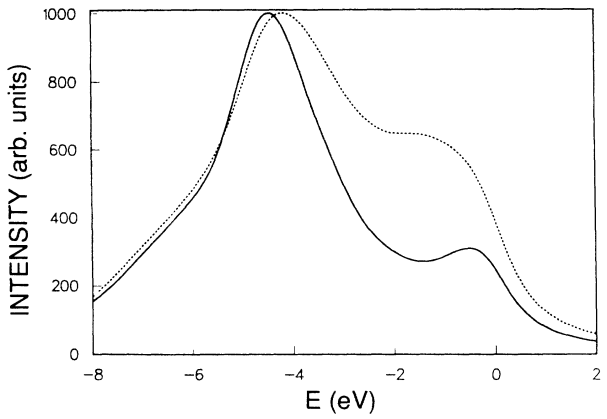

FIG. 9. Theoretical XPS spectra for TaC (solid line) and $TaC_{0.72}$ (dotted line). E_F is at 0.

-1.3 eV (B') for the substoichiometric compound (Fig. 9, dashed line). In Table II we list energy differences between the different peaks in the experimental and theoretical spectra. We find that the largest deviation between experiment and theory is 0.5 eV. These differences may be due to the use of the local-density-functional approximation for calculating the excited states and also to effects like background and surface scattering. The differences in the intensities between experiment and theory appear to be due to background scattering which is not included in our calculation. Looking at -8 eV we find a difference in the intensities of about 200 (arbitrary units) which can roughly be found across the whole spectrum. But more or less all the features which are found in the experimental curves are also seen in the theoretical ones. We can now assign each peak in the spectrum. The main peak (A) around -4.5 eV is built up mainly from Ta $5d$-like contributions. Since there is strong hybridization (for the stoichiometric as well as the substoichiometric compound) with C p states it cannot be labeled as only Ta $5d$. The second peak (B) around -1.0 eV is only Ta $5d$-like in both cases. As was discussed earlier, it is the charge transferred back from the carbon to the tantalum that gives rise to this increased intensity in the XPS spectrum in the substoichiometric compounds in this energy region.

TABLE II. Peaks in the experimental (Ref. 8) and calculated XPS spectrum of TaC_x in eV. The Fermi energy is at 0.0. Also listed are energy differences between the different peaks. The largest deviation between experiment and theory is 0.7 eV. x is the concentration.

x	Peaks	Experiment	Theory
1.00	A	-5.28	-4.55
	B	-0.97	-0.5
0.72	A'	-4.8	-4.2
Energy	B-A	4.4	3.95
differences	A'-A	0.5	0.3

VI. DISCUSSION

In contrast to previous findings for substoichiometric TiN_x (Ref. 1) and other similar compounds,[2,3] we do not find any significant vacancy contributions to the DOS in TaC_x. In order to understand this we performed the same analysis for a single vacancy impurity as is described by Klima *et al.*[1] [especially Fig. 2 and Eq. (29) therein]. In the case of TaC we find that below E_F this resonance condition is not fulfilled. The real part of the scattering path operator $\tau^{00}_{\Gamma_6^+}(E)$ is positive below E_F whereas the impurity matrix is negative. Therefore even for a zero-vacancy potential the resonance condition cannot be fulfilled. Therefore we find only weak scattering in the vicinity of the vacancy and no virtual bound states in the energy region of interest.

Creating vacancies does cause a charge transfer back from the carbon atoms to the tantalum atoms (see Table I) in TaC_x. As was discussed in Ref. 9 this charge transfer can be understood in the following way. We find hybridization between the C $2p$-like states and the Ta $5d$-like states around -4.5 eV in the DOS of the stoichiometric compound. In a tight-binding picture one can say that the atomiclike energy positions of the Ta $5d$ states are lowered with respect to the C $2p$ states as understood in terms of bonding and antibonding states. Removing now part of the carbon atoms means some of the metal–nonmetal bonds are also removed and there is now less hybridization. Therefore part of the Ta $5d$-like states which can no longer form a hybrid with C $2p$ states are found at higher energies around -1.0 eV as $5d(\Gamma_7^+)$-like states. This charge transferred back into these states is in agreement with the calculation by Klein *et al.*[9] and indicates their explanation of the changes in the electronic structure is basically correct.

In a simple theory the linear specific-heat coefficient γ is given by the DOS at the Fermi energy. We list the DOS at E_F in Table I. We find a slight decrease in the DOS (at E_F) in going from TaC to $TaC_{0.72}$. Even taking electron-phonon enhancement into account as described in Ref. 9 cannot explain the experimental findings of a rather big drop in γ. This discrepancy between experiment and theory may be due to unusual phonon effects caused by the carbon vacancies. A calculation of the phonon spectrum in the sense of Varma *et al.*[22,23] would be helpful to understand this behavior.

As was discussed already, the XPS experiment mainly sees the $5d$-like tantalum contributions. The changes between 1 and 2 eV below E_F are only due to the charge transferred back from the carbon atom to the metal and not to additional vacancy states. Small contributions to the vacancy states are found around -3.0 eV and do not show up in the spectrum. The other change in the experimental spectrum going from stoichiometric TaC to substoichiometric TaC_x is a shift of the main peak towards the Fermi energy. This shift of E_F towards lower energies with increasing vacancy concentration is due to the charge found around the vacancy. Although the vacancy states are not seen directly by the XPS experiment this small amount of charge lowers E_F and causes the peaks in the XPS spectrum to shift towards the Fermi energy. The DOS based on the tight-binding CPA calculation showed that the position of the main peak moves away from the Fermi energy with increasing vacancy concentration. That is because no vacancy states are found. This indicates that while the tight-binding CPA method gets some of the features right (like the charge transfer) it misses important changes. The question about metal vacancies remains to be looked at. From the experimental data it seems that they play no or a rather unimportant role.

In conclusion we can say that the creation of additional vacancy states in TaC_x leads to different effects than seen in the lighter carbide and nitride intermetallics. The main mechanism for the change in the electronic structure of TaC_x is a charge transfer back from the nonmetal to the metal with increasing vacancies in agreement with the earlier argument based on a tight-binding CPA calculation.[9] However, the additional vacancy states around -3.0 eV are the reason for a lower E_F in the substoichiometric compounds. The features seen in the XPS spectrum are mainly due to the $5d$ electrons of tantalum, because of their large cross sections and large DOS contributions. With increasing vacancy concentration we find that the charge transferred to the tantalum atom shows up in the XPS spectrum at $5d(\Gamma_7^+)$-like states around 1–2 eV below E_F. The shift of the Fermi energy to lower energies with increasing vacancies shows up in the experimental as well as the theoretical XPS spectra as a shift of the main peak towards E_F. This reasonably good agreement between experiment and theory is a pleasant surprise as our RKKR CPA calculation is not done self-consistently with respect to the one-electron charge density and despite the fact that we are treating the excited states within the density-functional theory. The experimental linear specific-heat coefficient which decreases with increasing vacancy concentration cannot be explained simply from the change in the DOS at the Fermi energy. A self-consistent calculation may bring better agreement between the theoretical and experimental XPS spectra, but certainly cannot explain the behavior of the linear specific-heat coefficient.

ACKNOWLEDGMENT

One of us (P.W.) wants to acknowledge a grant by the Austrian National Bank (Project No. 3048). This work was performed under the auspices of the U.S. Department of Energy.

[1] J. Klima, G. H. Schadler, P. Weinberger, and A. Neckel, J. Phys. F **15**, 1307 (1985).

[2] P. Marksteiner, P. Weinberger, A. Neckel, R. Zeller, and P. H. Dederichs, Phys. Rev. B **33**, 812 (1986).

[3] J. Redinger, R. Eibler, P. Herzig, A. Neckel, R. Podloucky, and E. Wimmer, J. Phys. Chem. Solids **46**, 383 (1985).

[4] See Refs. in Ref. 8.

[5] J. Pfueger, J. Fink, G. Crecelius, K. P. Bohnen, and H. Winter,

Solid State Commun. **44**, 489 (1982).
[6]V. A. Gubanov, E. Z. Kurmaev, and D. E. Ellis, J. Phys. **14**, 5567 (1981).
[7]H. Höchst, P. Steiner, S. Hüfner, and C. Politis, Z. Phys. B **37**, 27 (1980).
[8]G. R. Gruzalski and D. M. Zehner, Phys. Rev. B **34**, 3841 (1987).
[9]B. M. Klein, D. A. Papaconstantopoulos, and L. L. Boyer, Phys. Rev. B **22**, 1946 (1980).
[10]L. E. Toth, *Transition Metal Carbides and Nitrides* (Academic, New York, 1971).
[11]J. Staunton, B. L. Gyorffy, and P. Weinberger, J. Phys. F **10**, 2665 (1980).
[12]P. Weinberger, J. Staunton, and J. L. Gyorffy, J. Phys. F **12**, 2229 (1982).
[13]G. H. Schadler, P. Weinberger, A. Gonis, J. Klima, J. Phys. F **15**, 1675 (1985).
[14]P. Weinberger and A. Gonis, *Handbook of the Physics and Chemistry of the Actinides* (North-Holland, New York, 1987), Vol. 5.
[15]Y. Onodera and M. Okazaki, J. Phys. Soc. Jpn. **21**, 1273 (1966).
[16]B. Segall, Phys. Rev. **105**, 108 (1956).
[17]J. S. Faulkner, Prog. Mater. Sci. **27**, 1 (1982).
[18]P. Marksteiner, P. Weinberger, R. C. Albers, A. M. Boring, and G. H. Schadler, Phys. Rev. B **34**, 6730 (1986).
[19]W. H. Fehlner and S. H. Vosko, Can. J. Phys. **54**, 2159 (1976).
[20]P. Weinberger, R. Podloucky, C. P. Mallet, and A. Neckel, J. Phys. C **12**, 801 (1979).
[21]J. Redinger, P. Marksteiner, and P. Weinberger, Z. Phys. B **63**, 321 (1986).
[22]C. M. Varma, E. I. Blount, P. Vashista, and W. Weber, Phys. Rev. B **19**, 6130 (1979).
[23]C. M. Varma and W. Weber, Phys. Rev. B **19**, 6142 (1979).